International Journal of Thermal Sciences 48 (2009) 2249–2254

Contents lists available at ScienceDirect

International Journal of Thermal Sciences

journal homepage: www.elsevier.com/locate/ijts

Modified self-consisted scheme to predict the thermal conductivity of nanofluids

Kliment B. Hadjov*

University of Chemical Technology & Metallurgy, Kl. Ohridski blv. 8, 1756 Sofia, Bulgaria

ARTICLE INFO

Article history:
Received 15 September 2008
Received in revised form
24 May 2009
Accepted 25 May 2009
Available online 23 June 2009

Keywords:
Thermal conductivity
Nanofluids
Homogenization
Self-consistent scheme

ABSTARCT

In this study, the self-consisted scheme is generalized to predict the thermal conductivity of nanofluids containing spherical nanoparticles with a conductive interface. We assume a flux jump in the particle–fluid interface in the opposite to the assumption for temperature jump in the case of thermal barrier resistance. We have obtained an upper and lower bounds to the homogenized suspension thermal conductivity according to the particle packing, which is particle surface state dependent. A comparison with the Hashin–Shtrikman bounds and the Maxwell equation is made. The proposed model is evaluated using published experimental data of the thermal conductivity enhancement for different nanofluids.

1. Introduction

Nanofluids are colloidal fluidic systems containing nanosized particles at low volume fractions. They show unusually high thermal conductivities if prepared in a stable manner. The role of the particle interface concerning in thermal conductivity enhancement seems to be very important. There are different physical explanations related to the interfacial behaviour.

For suspensions at rest, the additional surface conductance has been studied by Rubio-Hernándes et al. [1]. They claim that a dynamic Stern layer based on the adsorbed ionic spaces on the particle surface may be responsible for viscosity effects in nano-suspensions and thus for the thermal conductivity behaviour.

Photon correlation spectroscopy has been employed by Bouclé et al. [2] to characterize various SiC suspensions, through the hydrodynamic diameters of particles in solution. These observations point out the key role played by the particle surface state, mainly dependant on the C/Si ratio and the polymeric dispersant.

Experimental data on the thermal conductivity enhancement of nanofluids from literature Zhang et al. [3] show an astonishing spectrum of results. A variety of theoretical models by Wang and Mujumder [4] try to explain the various experimental results. Because of the variety of data trends, there is always one data set which can be found to substantiate one model or another. These models often contain different parameters for which a reasonable measuring procedure does not exist. In this work we propose a model which takes into account the particle interface state. This model contains measurable parameters with physical meaning and gives the possibility to determine upper and lower bounds of the suspension thermal conductivity enhancement as a function of the particle concentration.

2. General framework

According to the traditional self-consistent scheme (SCS) [5] assuming noninteraction between inclusions, a spherical inclusion of radius a is embedded in a concentric sphere matrix material of radius b, which is embedded in an infinite effective medium possessing the unknown effective thermal conductivity k_{eff}. The ratio of the radii a/b relates the volume fraction of particles by $f=(a/b)^3$. The steady-state conduction equations of a particulate composite can be written as [5,6]

$$\begin{aligned} \nabla^2 T_{\text{p}} &= 0, \quad \text{if } 0 \le r \le a; \\ \nabla^2 T_{\text{f}} &= 0, \quad \text{if } a \le r \le b; \\ \nabla^2 T_{\text{eff}} &= 0, \quad \text{if } b \le r < \infty. \end{aligned} \tag{1}$$

Here T_{p}, T_{f}, T_{eff} are the temperature fields in the particles, the bulk fluid and in the effective area respectively; r is the radius variable in the spherical coordinate system (r, θ, φ).

* Tel.: +359 888996152.
E-mail address: klm@uctm.edu

1290-0729/$ – see front matter © 2009 Elsevier Masson SAS. All rights reserved.
doi:10.1016/j.ijthermalsci.2009.05.008

Nomenclature

a	spherical inclusion radius, m
b	radius of the concentric sphere matrix material, m
A_p, A_f	unknown parameters, K m^{-1}
B_f, B_{eff}	unknown parameters, K m^{-2}
f	volume fraction of particles, –
f_{max}	maximal particle packing, –
h	thermal barrier resistance parameter, W m^{-2} K^{-1}
k_{eff}	effective thermal conductivity, W m^{-1} K^{-1}
k_f, k_p	thermal conductivities of the bulk fluid and the particles, W m^{-1} K^{-1}
k_m	matrix conductivity, W m^{-1} K^{-1}
k	flux discontinuity parameter, –
$\Delta q(r=a)$	heat flux jump at the interface, W m^{-2}
$q_{eff}(\infty)$	heat flux at large distance from the particle, W m^{-2}
r	current radius, m
T_p, T_f, T_{eff}	temperature fields, K

Greek symbols

α	thermal conductivity ratio particle/base fluid (or matrix), –
$\beta=\nabla T_{eff,\infty}$	temperature gradient at large distance away from the particle, W m^{-1}
λ	phonon (electron) mean free path, m
θ, φ	angles of the spherical coordinate system, rad

To take into account the thermal barrier resistance, the authors in [6] and [7] assume a temperature jump between the inclusion and the matrix. We now assume, as proposed by Nan [7], a flux jump between the inclusion and the matrix. Thus, we take into account the so called thermal conductive interface (opposite to the thermal resistant interface), which can be related to the ordered liquid molecules at the interface possessing greater conductivity than the bulk liquid, or to the adsorbed ionic species at the particle surface, or to the hydrodynamic diameter of particles in solution due to the double solvation layers [2].

It is important to say that we do not consider the interfacial layer as a separate component in the suspension as the authors in [8] have made. Thus, we can take into account different physical reasons for the enhanced interface conduction. Now, the boundary conditions at the interfaces can be written as

$$T_p = T_f \quad \text{at } r = a, \tag{2.1}$$

$$k_f \nabla T_f = k_p \nabla T_p + k \cdot k_{eff} \beta \quad \text{at } r = a, \tag{2.2}$$

$$T_f = T_{eff} \quad \text{at } r = b, \tag{3.1}$$

$$k_f \nabla T_f = k_{eff} \nabla T_{eff} \quad \text{at } r = b, \tag{3.2}$$

where k_f, k_p, k_{eff} are the thermal conductivities of the bulk fluid, the nanoparticles and the effective medium respectively; k is a nondimensional flux discontinuity parameter which will be estimated later; $\alpha = k_p/k_f$ is the thermal conductivity ratio particle/base fluid; $\beta = \nabla T_{eff,\infty}$ is the temperature gradient at large distance away from the particle.

The relations in equations (2.1) and (3.1) express the temperature continuity across the interfaces, the relation in equation (3.2) expresses the heat flux continuity, while the relation in equation (2.2) expresses the heat flux jump (discontinuity) across the particle–matrix interface, which is taken to be proportional to the temperature gradient at large distances away from the particle. In the case of perfect particle/fluid contact the continuum mechanics involves a flux continuity across this interface. To take into account the enhanced conductivity of a negligible thin region surrounding the particle, at this interface we assume energy production in an other (small) scale, due to chemical reactions related for example with the suspension pH. In other words the interfacial thermal contact conductance in a composite can arise from an intensive chemical adherence at the interface. In the case of perfect contact between particle and matrix (without thermal conductive interface) the parameter k should be zero.

The temperature field solutions are taken in the form proposed by Leong et al. [9] and Tihonov and Samarskii [10]

$$T_p = A_p r \cos\theta, \quad 0 \le r \le a; \tag{4.1}$$

$$T_f = \left(A_f r + B_f / r^2\right) \cos\theta, \quad a \le r \le b; \tag{4.2}$$

$$T_{ef} = \beta r \cos\theta, \quad b \le r < \infty. \tag{4.3}$$

Here A_p, A_f and B_f are the integration constants. Following [10], the first equation concerns an internal problem, the second one an intermediate problem and the third one an internal problem, because of the limited particle concentration. The authors in [6] have demonstrate that even using an intermediate representation to the equation (4.3) $T_{eff} = (\beta r + B_{eff}/r^2)\cos\theta$ as usual [5], in the case of discontinuity at the particle–matrix interface, the coefficient $B_{eff} = 0$.

Substitution of equations (4) into equations (3) becomes

$$\begin{aligned} &a^3 A_p - a^3 A_f - B_f = 0, \\ &a^3 k_p A_p - a^3 k_f A_f + 2 k_f B_f = -a^3 k \cdot k_{eff} \beta, \\ &b^3 A_f + B_f = b^3 \beta, \\ &b^3 k_f A_f - 2 k_f B_f = b^3 k_{eff} \beta. \end{aligned} \tag{5}$$

Equations (5) represent a linear system to obtain the unknown parameters A_p, A_f, B_f and the effective thermal conductivity k_{eff}. After some algebraic transformations, solving the system (5) to the relative effective thermal conductivity we can write

$$k_{eff}/k_f = \frac{2 + \alpha + 2(\alpha - 1) f}{2 + \alpha - (\alpha - 1) f - 3 k \alpha f}. \tag{6}$$

The Maxwell equation to the relative effective conductivity of two phase particulate composites can be expressed as follows [11]

$$k_{eff}/k_f = \frac{2 + \alpha + 2(\alpha - 1) f}{2 + \alpha - (\alpha - 1) f}. \tag{7}$$

It is obviously clear, that in the case of simple perfect contact without interface (ordered fluid layer) conductivity $k = 0$. In this case equations (6) and (7) coincide.

To obtain the flux discontinuity parameter k, we make the following change. In equation (6) we replace f with the maximal real particle packing f_{max} and k_{eff}/k_f with the maximal possible relative thermal conductivity enhancement $\alpha = k_p/k_f$ respectively. Thus, after transformation we obtain

$$k = \frac{(1 + \alpha - 2/\alpha)\,(1 - f_{max})}{3 \alpha f_{max}}. \tag{8}$$

The maximal packing f_{max} for different suspension morphologies are well known and can be found in Nielsen [12]. Theoretically the maximum value of f_{max} is 0.7405 for spheres in hexagonal close packing, but in practice f_{max} should be closer to 0.6370

(random close). The minimal value of f_{max} should be equal to 0.5236 (simple cubic). Practically f_{max} varies with particle shape and state of agglomeration. Except in a few cases, it is difficult to predict the kind of the particle packing from theory, so an experimental method such as sedimentation volume can be used. Agglomerates and nonspherical particles generally have smaller f_{max} than spheres [12]. On the other hand the particle surface state (the interface behaviour) may be in part responsible for the suspension morphology. Moreover, from equation (8) we can obtain the following results as limit cases ($\alpha \to 1$ and $\alpha \to \infty$)

$$k = 0, \tag{9.1}$$

and

$$k = \frac{1 - f_{max}}{3 f_{max}}. \tag{9.2}$$

The first result indicates that in the case of a small difference between the inclusion and bulk fluid suspension, conductivities obey the Maxwell equation (7). From equation (2.2), we have $\Delta q(r = a) = k q_{eff}(\infty)$. Making the assumption that the heat flux jump at the interface, $\Delta q(r = a)$, do not exceed the heat flux at a large distance, $q_{eff}(\infty)$, we obviously should have $k = 1$. Now, from equation (9.2) to the maximal packing value we obtain $f_{max} = 0.25$. Thus, practically for real nanosuspensions we can write

$$0.25 \le f_{max} \le 0.637. \tag{10}$$

Using the inequality (10), our equations (6) and (8) form upper and lower bounds to the thermal conductivity enhancement of nanosuspensions. As one can see, these bounds are able to describe the experimental results obtained by the researchers and are closer than the Hashin–Shtrikman ones employed by Keblinski et al [13]. Fig. 1 illustrates the flux discontinuity parameter k as a function of the thermal conductivity ratio $\alpha = k_p/k_f$, (particle to base fluid), for two maximal packings. Fig. 2 illustrates the same parameter as a function of the maximal particle packing f_{max} for $\alpha = 69$. Both figures concern aluminium oxide particles in water according to the inequality limits in equation (10). The respective theoretical curves in both figures are plotted according to equation (8).

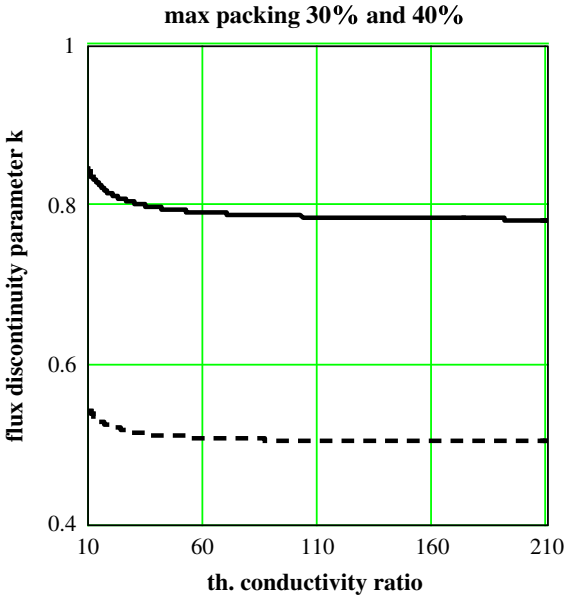

Fig. 1. Flux discontinuity parameter $k(\alpha)$. Continuous line $f_{max} = 0.3$, dashed line $f_{max} = 0.4$.

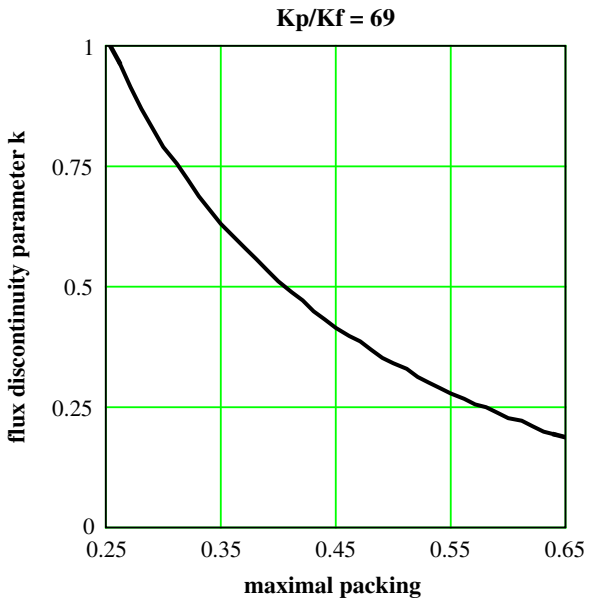

Fig. 2. Flux discontinuity parameter $k(f_{max})$ for Al_2O_3 & water. $\alpha = 69$.

One can see that k remains practically independent from the thermal conductivity ratio α, which for nanosuspensions is greater than 50. On the other hand, this parameter is strongly dependent from the maximal particle packing (the suspension morphology).

Using a similar SCS approach Lee et al. [6] have obtained an equation (see below) concerning the thermal conductivity of composites assuming a temperature jump at the particle–matrix interface. Thus, they predict the homogenized conductivity for composites with a thermal barrier resistance at the interface. A modification of the Maxwell theory developed by Hasselman and Johnson [14] obtains the same expression. Both expressions can be written in the following form, which is easily comparable with our results,

$$k_{eff}/k_f = \frac{2 + \alpha + 2(\alpha - 1)f + 2\alpha(1 - f)K_m/ah}{2 + \alpha - (\alpha - 1)f + \alpha(2 + f)K_m/ah}. \tag{11}$$

Here k_m is the matrix conductivity, corresponding to k_f in our equations, $\alpha = k_p/k_f$ and h is the thermal barrier resistance parameter. For $h \to \infty$ one obtains the Maxwell equation (7). Equations (6), (8) and (11) on the other hand are compared in Fig. 3. Note that our equations (6) and (8) for $k \to 0$ also coincide with Maxwell's. Thus, the Maxwell equation is the upper limit for the Hasselman–Lee equation (11) in the case of perfect interfacial contact. Conversely, the lower limit of our equations (6) and (8) can be obtained with $f_{max} = 0.637$, corresponding to the random close packing, which seems to be the maximal possible limit; the lower limits do not coincide with the Maxwell equation – see Figs. 4–6. If we deal with micro particles, f_{max} can be even greater (close to 1 in the case of multi sized particle distribution as discussed by Hashin [5]), and the Maxwell prediction can be reached.

Remark: The general opinion about the particle size influence on the nanosuspensions thermal conductivity is that the conductivity increases with decreasing the size [15]. Equations (6) and (8) do not take into account the particle size directly. According to Xie et al. [16] there are two size factors responsible for the thermal conductivity enhancement. First, heat transfer between the particle and the fluid takes place at the particle–fluid interface. Reduction in particle size can result in a large interfacial area. Second, the phonon (electron) mean free path λ for nonmetallic (metallic) inclusions, in the case of small particles, can be comparable to the

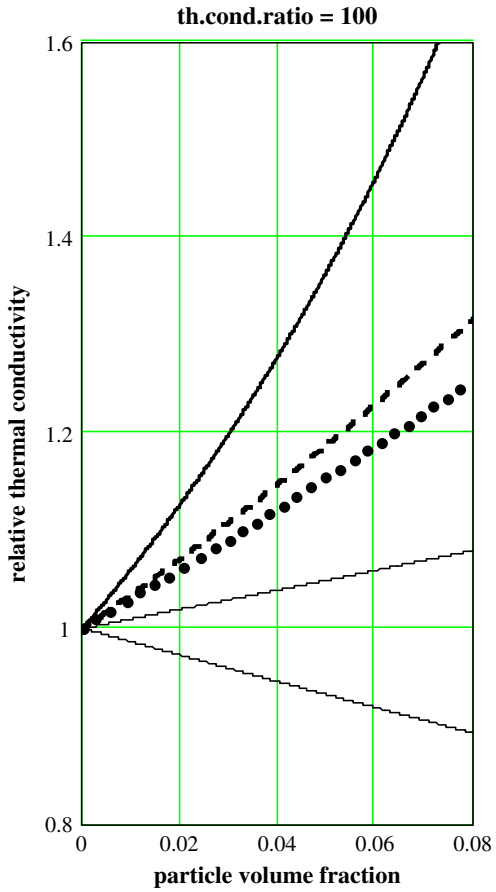

Fig. 3. Relative thermal conductivity enhancement for $\alpha = 100$. Thick continuous line – $f_{max} = 0.25$, dashed line – $f_{max} = 0.637$; both lines – equations (6) and(8). Dotted line – Maxwell equation (7). Thin lines: equation (11). $k_m/ah = 20$ – lower line, $k_m/ah = 0.4$ – upper line.

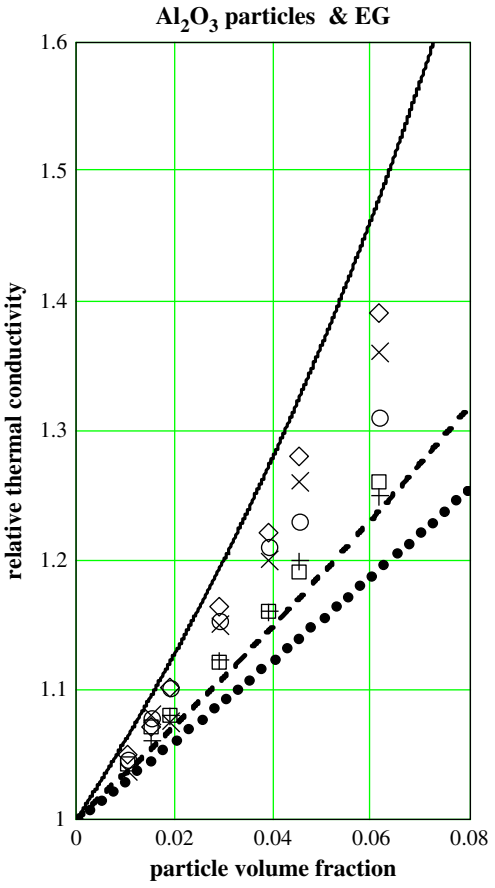

Fig. 4. Relative thermal conductivity enhancement for Al_2O_3 in EG. Continuous line – upper bound for $f_{max} = 0.25$, dashed line – lower one for $f_{max} = 0.637$; both lines from equations (6) and (8); dotted line – Maxwell equation (7). Experimental data – Kabelac and Kuhnke [19].

size of the particles (for aluminium oxide and cuprum oxide, λ is estimated to be around 35 nm [17]). The intrinsic conductivity of the particle may be reduced due to the scattering of the primary carriers of energy at the particle boundary. In this second case, the conductivity will be reduced with an increase in the particle surface. Therefore, for a suspension with particle sizes greater than the phonon (electron) mean free path, the conductivity increases when the particle size decreases (the first factor is dominant). Reciprocally, when the particle size is smaller than the mean free path, the second factor would govern the mechanism of the suspension conductivity. But in the last case (very small particles) the Brownian motion induced convection plays an important role and enhances the nanosuspensions conductivity [18]. Thus explains the seemingly contradictory experimental results as indicated by Kabelac and Kuhnke [19]. Our model takes into account the particle size via the maximal packing, which is size distribution dependent.

3. Experimental comparisons

Here we compare the predictions of our model, according to equations (6) and (8), with the experimental data from many authors systematized by Kabelac and Kuhnke [19]. A comparison between our equations (6) and (8) and the Hasselman–Lee model, equation (11), is illustrated for thermal conductivity ratio $\alpha = k_p/k_f = 100$ in Fig. 3. The conductivity enhancement according to our model with $f_{max} = 0.25$, 0.637 and the Maxwell equation (7) are plotted with continuous, dashed and dotted lines respectively. In this figure, we illustrate also equation (11) with thin lines for two different values of the thermal barrier resistance parameter h as mentioned in Fig. 3.

Experimental values for ethylene glycol (EG) with aluminium oxide (Al_2O_3) nanoparticles from different authors are plotted with different symbols from [19] in Fig. 4. Our upper and lower bounds according to equations (6) and (8) together with (10) are also plotted.

In Figs. 5 and 6 we compare our model (continuous lines) predictions with experimental data for Al_2O_3 and cuprum oxide (CuO) particles in water respectively, systematized by Kabelac and Kuhnke [19]. In Fig. 5 we have plotted the Hashin–Shtrikman (H.S.) bounds [5]. The lower H.S. bound coincides with the Maxwell equation. One can see that our bounds are closer to the experimental results. The same conclusion concerning the H.S. bounds can be made if we put them in Figs. 4 and 6. Note that in [13] Keblinski has demonstrated that the H.S. bounds are large to well describe the experimental results.

In Figs. 4–6 experimental data are plotted with different symbols from different authors.

In Figs. 3–6 the lower dotted line corresponds to the classical Maxwell model – equation (7). From these figures one can see that all experimental data take place between our bounds. Strictly speaking in the case of large size particle distribution, f_{max} can be greater than 0.637 and stay closer to 1 which transforms our model into the Maxwell one.

Moreover, recently in the case of small particles, Chen et al. in [20] have used small angle X-ray scattering to characterize the

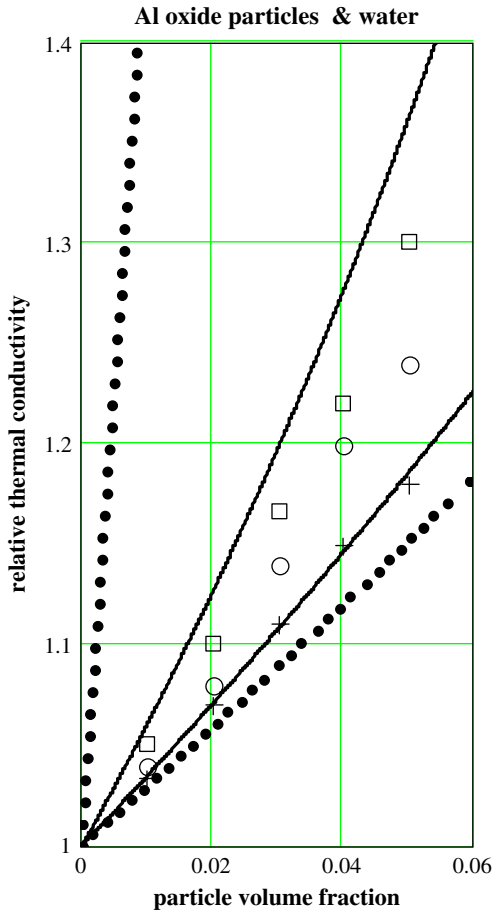

Fig. 5. Al_2O_3 particles in water. Upper line – $f_{max} = 0.25$, lower line – $f_{max} = 0.637$. Dotted lines – upper and lower H.S. bounds. The lower one coincides with the Maxwell equation (7). Experimental data – Kabelac and Kuhnke [19].

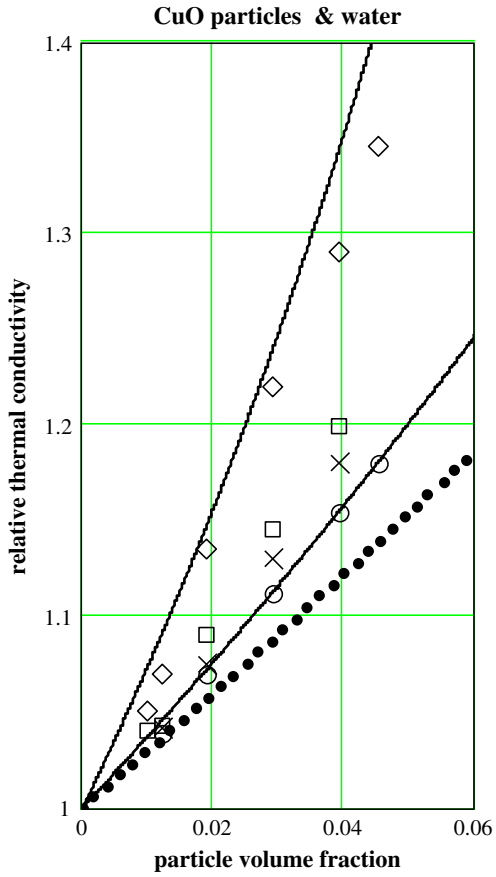

Fig. 6. CuO particles in water. Upper line – $f_{max} = 0.25$, lower line – $f_{max} = 0.637$. Dotted line – Maxwell equation (7). Experimental data – Kabelac and Kuhnke [19].

particle size in silica nanofluids. It was found that the particles in these fluids are monodispersed with average sizes between 10 and 30 nm (shorter than the phonon mean free path). Thermal conductivity measurements of 16 vol.% nanofluids with different sizes show a linear increase with increasing particle size. This result contradicts theoretical models based on fluid interfacial layer or Brownian motion because these models do not take into account the inclusion mean free path limit discussed above and the influence of the particle interface state.

Maximal conductivity enhancement can be expected if the average particle size is equal or smaller than λ and the particle size distribution possesses a lower standard deviation (particles with similar sizes). In this case ($2a \leq \lambda$), f_{max} reaches its minimal value of 0.25. If $2a \gg \lambda$ and the size deviation becomes larger (particles with different sizes as the SCS assumes to obtain the Maxwell equation), then f_{max} reaches its maximal value 0.637 or eventually a greater value if the particle size distribution is very large and a greater packing is possible. If $2a \ll \lambda$, f_{max} becomes greater, but due to the Brownian motion, which in this case (very small particles) can not be neglected, we should not expect an essential reduction of the suspension thermal conductivity.

Clustering can also decrease the maximal packing and enhance the conductivity [21]. Increasing difference of the pH values between suspension and particles isoelectric point increase the repulsive hydration forces among particle [15] and thus decrease the f_{max}. The experimental results from many authors, systematized by Kabelac and Kuhnke [19], are in good agreement with our model predictions. A slight nonlinearity is observed in the theoretical thermal conductivity enhancement with respect to particle volume fraction, even with small concentrations.

4. Conclusions

As one can see, the present model assumes a flux discontinuity at the phase interface due to the ordered fluid molecules at the particle–fluid border. Thus, the model proposed takes into account the enhanced conductivity of the interfacial layer without including the thermal conductivity and thickness of this thin layer. The suspension thermal conductivity is morphology dependent via the kind of particle packing. This packing depends on the particle surface state and size distribution. The limits of this packing parameter involve an upper and lower bounds of the effective suspension thermal conductivity. The experimental comparisons show that the proposed model well describes the limits of the conductivity enhancement with respect to the particle volume fraction for different nanosuspensions. In a consecutive work we will examine how the particle size distribution and suspension pH influence the nanofluid morphology via the maximal packing f_{max}.

Acknowledgements

Financial support by the AUF (project No 6316 PS 821/2008) is greatly acknowledged. The author would like to thank prof. A. Kassiba from the University of Maine (Le Mans – France) for the helpful discussions.

References

[1] F.R. Rubio-Hernández, Ruiz-Reina, A. Gómez Merino, The additional surface conductance: its role in the primary electroviscous effect, Colloids Surf. A 192 (2001) 349–356.

[2] J. Bouclé, N. Herlin-Boime, A. Kassiba, Influence of silicon and carbon excesses on the aqueous dispersion of SiC nanocrystals for optical application, J. Nanoparticle Res. 7 (2005) 275–285.

[3] X. Zhang, H. Gu, M. Fujii, Experimental study of the effective thermal conductivity and diffusivity of nanofluids, Int. J. Thermophys. 27 (2) (2006) 569–580.

[4] X.Q. Wang, A.S. Mujumder, Heat transfer characteristics of nanofluids: a review, Int. J. Therm. Sci. 46 (2007) 1–19.

[5] Z. Hashin, Assessment of the self consistent scheme approximation: conductivity of particulate composites, J. Comp. Mater. 2 (3) (1968) 284–300.

[6] Y.M. Lee, R.B. Yang, S.S. Gau, A generalized self-consistent method for calculation of effective thermal conductivity of composites with interfacial contact conductance, Int. Commun. Heat Mass Transf. 33 (2006) 142–150.

[7] C.W. Nan, R. Birringer, D.R. Clarke, H. Gleiter, Effective thermal conductivity of particulate composites with interfacial thermal resistance, J. Appl. Phys. 8 (10) (1997) 6692–6699.

[8] W. Yu, S.U.S. Choi, The role of the interfacial layers in the enhanced thermal conductivity of nanofluids, J. Nanoparticle Res. 6 (2004) 167–171.

[9] K.C. Leong, C. Yang, S.M.S. Murshed, A model for the thermal conductivity of nanofluids – the effect of interfacial layer, J. Nanoparticle Res. 8 (2006) 245–254.

[10] A.N. Tihonov, A.A. Samarskii, Equation of the Mathematical Physics, fourth ed. Nauka, Moskow, 1972, p. 735.

[11] J. Maxwell, A Treatise of Electricity and Magnetism, third ed. Clarendon, Oxford, 1904, p. 254.

[12] L.E. Nielsen, Mechanical Property of Polymers and Composites, second ed. M. Dekker, 1974, p. 382.

[13] P. Keblinski, R. Prasher, J. Eapen, Thermal conductance of nanofluids: is the controversy over? J. Nanoparticle Res. 10 (2008) 1089–1097.

[14] D.P.H. Hasselman, L.F. Johnson, Effective thermal conductivity of composites with interfacial thermal barrier resistance, J. Comp. Mater. 21 (1987) 508–514.

[15] S.P. Jang, S.U.S. Choi, Role of Brownian motion in the enhanced thermal conductivity of nanofluids, Appl. Phys. Lett. 84 (2004) 4316–4318.

[16] H. Xie, J. Wang, T. Xi, Y. Liu, F. Ai, Q. Wu, Thermal conductivity enhancement of suspensions containing nanosized alumina particles, J. Appl. Phys. 91 (2002) 4568–4572.

[17] K.S. Hwang, J.H. Lee, S.P. Jang, Buoyancy-driven heat transfer of water based Al_2O_3 nanofluids in a rectangular cavity, Int. J. Heat Mass Transf. 50 (2007) 4003–4010.

[18] J. Koo, C. Kleinstreuer, Impact analysis of nanoparticle motion mechanisms on the thermal conductivity of nanofluids, Int. Commun. Heat Mass Transf. 32 (2005) 1111–1118.

[19] S. Kabelac, J.-F. Kuhnke, Keynote lecture – convective heat transfer performance of nanofluids, in: Proceedings of the 13th ITHC, Sidney, Australia, 2006, pp. 1–33.

[20] G. Chen, W. Yu, D. Singh, D. Cookson, J. Routbort, Application of SAXS to the study of particle size dependent thermal conductivity of silica nanofluids, J. Nanoparticle Res. 10 (2008) 1109–1114.

[21] J.A. Eastman, S.R. Phillpot, S.U.S. Choi, P. Keblinski, Thermal transport in nanofluids, Annu. Rev. Mater. Res. 34 (2004) 219–224.